Waveguide Grating Filters for Dispersion Compensation and Pulse Compression

Jose E. Roman and Kim A. Winick, *Member, IEEE*

***Abstract*—Dispersion compensation and pulse compression is theoretically demonstrated using aperiodic waveguide gratings. The gratings are designed to have both a flat amplitude and a quadratic phase response over the pulse bandwidth. This results in nearly transform-limited compressed pulses. The appropriate waveguide grating parameters are obtained by applying the Gel'fand-Levitan-Marchenko inverse scattering method to the coupled mode equations which describe propagation. The technique is illustrated by designing an aperiodic grating, which compresses a 60 ps pulse by a factor of three. Limitations and possible extensions of the general method are discussed.**

I. Introduction

In long distance optical communication systems, fiber group velocity dispersion degrades system performance by either limiting the maximum data rate or by requiring a shorter distance between repeaters. These limitations can be particularly serious for systems operating at 1.5 μm, where large fiber dispersion values of 15 to 20 ps/km/nm, are typical. With a fiber dispersion value of 20 ps/km/nm for example, the width of a 20 ps Gaussian pulse will increase to 60 ps over a propagation distance of only 17 km. Group velocity dispersion (GVD) can be modeled as a frequency-dependent quadratic phase shift. Therefore, dispersion-induced effects may be eliminated, in principle, by using dispersion-compensating devices at the end of the fiber link. These devices must exhibit a quadratic phase shift over frequencies, which span the entire pulse bandwidth. Furthermore, the shift must be opposite in sign to the fiber GVD so the two effects cancel. It is also known that a quadratic phase shift can be used to compress linearly chirped pulses.

There are several well known techniques for producing frequency-dependent quadratic phase shifts. These include grating and prism pairs [1], Gires Tournois interferometers [2], and waveguide grating filters [3]–[7]. The dispersion of a grating pair is negative, and therefore it may only be used to compensate positive GVD. Unfortunately, fibers have negative GVD in the low loss wavelength region beyond approximately 1.3 μm. In addition, the required grating pair separation becomes extremely large when the pulsewidths are longer than tens of picoseconds. Finally, grating pairs are bulky and lossy. Gires Tournois interferometers can be realized as reflective Fabry–Perot etalons. Recently, partial dispersion compensation in a 5 Gb/s transmission system, operating at 1.5 μm, has been achieved using a reflective, fiber-pigtailed, Fabry–Perot, optical equalizer [8]. These devices can be made relatively small and compact. With the rear mirror reflectivity chosen to be 1, the Fabry–Perot has an all-pass frequency characteristic. The phase response is a function of the Fabry–Perot cavity spacing and the reflectivity of the front mirror. Both positive and negative GVD values can be realized by changing the cavity spacing. Gires Tournois interferometers, however, can only realize high levels of GVD over limited bandwidths. This fact severely compromises their ability to perform transform-limited pulse compression or dispersion compensation.

Waveguide grating filters have also been proposed for dispersion compensation and pulse compression. These devices are particularly appealing because of their small size and compatibility with fiber technology. Periodic waveguide gratings, however, suffer from the same problem as Gires Tournois interferometers. High GVD (either positive or negative) can be obtained, but only over a very limited bandwidth [9]. Ouellette [3]–[4] recently demonstrated that this bandwidth limitation may be removed by using a linearly chirped grating in place of a periodic structure.

This paper investigates the design of general aperiodic waveguide gratings for pulse compression and dispersion compensation. The Gel'fand–Levitan–Marchenko inverse scattering technique of quantum mechanics is used to design waveguide grating filters [10], [11]. These filters have nearly perfect frequency-dependent quadratic phase shifts over arbitrarily wide pulse bandwidths.

II. Theory of Pulse Compression and Dispersion Compensation

A. Dispersion Compensation

Consider a Gaussian pulse $x(t)$ which is centered at frequency ω_c

$$x(t) = \exp\left(-\frac{t^2}{2\tau_0^2}\right) \exp(j\omega_c t). \tag{1}$$

Manuscript received January 30, 1992; revised October 8, 1992. This work was supported by the NSF under Grant ECS-8909802 and through the Center for Ultrafast Optical Sciences under STCPHY8920108.

The authors are with the Department of Electrical Engineering and Computer Science, University of Michigan, Ann Arbor, MI 48109.

IEEE Log Number 9206533.

0018-9197/93$03.00 © 1993 IEEE

The Fourier transform $X(\omega)$ of this pulse can be computed using the following integral [12]

$$\int_{-\infty}^{\infty} \exp[-ax^2] \exp[-j(bx^2 + cx)]\, dx = \frac{\pi^{1/2}}{(a^2+b^2)^{1/4}} \exp\left[-\frac{ac^2}{4(a^2+b^2)}\right] \cdot \exp\left[-j\left(\frac{1}{2}\tan^{-1}\left(\frac{b}{a}\right) - \frac{bc^2}{4(a^2+b^2)}\right)\right] \quad (2)$$

where b and c are arbitrary constants and a is any positive real number. The result is

$$X(\omega) = \sqrt{2\pi\tau_0^2} \exp\left[-\frac{(\omega-\omega_c)^2\tau_0^2}{2}\right] \quad (3)$$

and full width half maximum bandwidth $\Delta\omega_{\mathrm{FWHM}}$ of the pulse is given by

$$\Delta\omega_{\mathrm{FWHM}} = (2(\ln 2)^{1/2})/\tau_0.$$

The pulse passes through a fiber of length L, which has dispersion $d^2\beta/d\omega^2 = 2\alpha$ at frequency ω_c. Thus, the fiber can be modeled (approximately) as a linear, time-invariant filter with transfer function

$$H(\omega) = \exp[-j\alpha L(\omega-\omega_c)^2] \qquad \omega > 0. \quad (4)$$

At the end of the fiber the Fourier transform of the output pulse $y(t)$ is

$$Y(\omega) = H(\omega)X(\omega). \quad (5)$$

Therefore,

$$y(t) = A \exp\left(-\frac{\tau_0^2 t^2}{2s}\right) \exp\left(j\frac{\alpha L t^2}{s}\right) \exp(j\omega_c t) \quad (6)$$

where

$$s = 4[(\tau_0^2/2)^2 + (\alpha L)^2] \quad (7)$$

and

$$A = \frac{\tau_0}{s^{1/4}} \exp\left[-j\frac{1}{2}\tan^{-1}\left(\frac{2\alpha L}{\tau_0^2}\right)\right]. \quad (8)$$

It follows from (1) and (7) that the pulsewidth has been increased by a factor of C_d, where

$$C_d = \left[1 + \left(\frac{2\alpha L}{\tau_0^2}\right)^2\right]^{1/2}. \quad (9)$$

If $y(t)$ is to be compressed back to its original width, then it must be placed through a compression filter having transfer function

$$H_d^{opt}(\omega) = H^{-1}(\omega) = \exp\left[j\frac{(C_d^2-1)^{1/2}}{2}\tau_0^2(\omega-\omega_c)^2\right] \qquad \omega > 0. \quad (10)$$

Equation (10) must be satisfied over those frequencies, which lie within the pulse bandwidth.

B. Pulse Compression

Consider the compression of a linearly chirped pulse $w(t)$ centered at frequency ω_C

$$w(t) = \exp\left(-\frac{t^2}{2\tau_0^2}\right) \exp(j\theta t^2) \exp(j\omega_c t). \quad (11)$$

In practice, the linear chirp could be produced by self-phase modulation in an optical fiber. The Fourier transform of $w(t)$ can be found using (2), and the result is

$$W(\omega) = B \exp\left[-\frac{(\omega-\omega_c)^2\tau_0^2}{2u}\right] \cdot \exp\left[-j\frac{\theta\tau_0^4(\omega-\omega_c)^2}{u}\right] \quad (12)$$

where

$$u = [1 + 4(\theta\tau_0^2)^2] \quad (13)$$

and

$$B = \frac{\sqrt{2\pi}}{u^{1/4}}\tau_0 \exp\left[j\frac{1}{2}\tan^{-1}(2\theta\tau_0^2)\right]. \quad (14)$$

It follows from (12), that a compressed transform-limited pulse will be obtained if $w(t)$ is placed through a filter having transfer function

$$H_c^{opt}(\omega) = \exp\left[j\frac{\theta\tau_0^4(\omega-\omega_c)^2}{u}\right] \qquad \omega > 0. \quad (15)$$

In the frequency domain the compressed pulse $v(t)$ will then be given as

$$V(\omega) = W(\omega)H_c^{opt}(\omega). \quad (16)$$

Therefore, using (2),

$$v(t) = D \exp\left[-\frac{t^2}{2\tau_0^2/u}\right] \exp(j\omega_c t) \quad (17)$$

where

$$D = u^{1/4} \exp[j\tfrac{1}{2}\tan^{-1}(2\theta\tau_0^2)]. \quad (18)$$

It follows from (11), (13) and (17) that the compression ratio C_c is

$$C_c = \sqrt{u} = [1 + 4(\theta\tau_0^2)^2]^{1/2} \quad (19)$$

and thus

$$H_c^{opt}(\omega) = \exp\left[j\frac{(C_c^2-1)^{1/2}}{2}\tau_f^2(\omega-\omega_c)^2\right] \qquad \omega > 0 \quad (20)$$

where

$$\tau_f = \frac{\tau_0}{C_c}. \quad (21)$$

Thus, the required filter transfer function for either pulse compression or dispersion compensation is given by (20). C_c is the desired compression ratio, and τ_f is the $1/e$ intensity point of the Gaussian pulse following compression. We note that the if filter transfer function $H_c(\omega)$ is multiplied by any linear phase term, $\exp[-j(a\omega + b)t]$, then the basic result remains unchanged. The compressed pulse is simply delayed in time.

In the remainder of this paper, pulse widths and bandwidths will be specified in terms of the separation between half maximum intensity points. Thus, the pulse described by (1) and (3) has width and bandwidth given by $2(\ln 2)^{1/2}\tau_0$ and $2(\ln 2)^{1/2}/\tau_0$, respectively.

III. Filters with Rational Representations

It is impractical to design filters which have infinite bandwidth. Thus, we consider the effect of cascading the optimum compression filter $H_c^{opt}(\omega)$ with a first-order Butterworth. The transfer function of the two-filter cascade is

$$H_c(\omega) = \frac{1}{1 + j(\omega - \omega_c)/\omega_0} H_c^{opt}(\omega) \tag{22}$$

and it has a 3 dB bandwidth equal to $2\omega_0$. It is a straightforward exercise to show (see Appendix A) that the compressed pulse $v(t)$ now becomes

$$v(\tau) = D\sqrt{\frac{\pi}{2}}\,\alpha_0 \exp(\alpha_0^2/2)\exp(-\alpha_0\tau) \cdot \left[1 + \operatorname{erf}\left(\frac{\tau - \alpha_0}{2^{1/2}}\right)\right]\exp(j\omega_c\tau\tau_f) \tag{23}$$

where

$$\alpha_0 = \omega_0\tau_f = \sqrt{\ln 2}\,\frac{BW_f}{BW_p} \tag{24}$$

$$\tau = t/\tau_f \tag{25}$$

$$\operatorname{erf}(x) = \frac{2}{\sqrt{\pi}}\int_0^x \exp(-y^2)\,dy. \tag{26}$$

In (24) BW_p and BW_f are he 3 dB bandwidths of the transform-limited compressed pulse and the compression filter, respectively. The degradation in compressed pulse shape, due to the insertion of the Butterworth filter (with $\alpha_0 = 2(2)^{1/2}$), is illustrated in Fig. 1. Note that in Fig. 1 the center of the pulse is offset from the point $t = 0$. This offset occurs because the Butterworth filter has phase delay. For comparison purposes, the pulse from the ideal compressor has also been plotted using the same time offset. A calculation shows that the Butterworth filter reduces the pulse energy by only 5%. In a subsequent design example, BW_f/BW_p will be chosen to be 3.4 (i.e., $\alpha_0 = 2(2)^{1/2}$), and as Fig. 1 illustrates, the resulting degradation will be small.

In filter design it is often useful to approximate a transfer function by a rational representation in the s-plane

$$H_c^{opt}(s) \approx H_c(s) = k\frac{\prod_{i=1}^{M}(s - z_i)}{\prod_{i=1}^{N}(s - p_i)}, \quad M \le N. \tag{27}$$

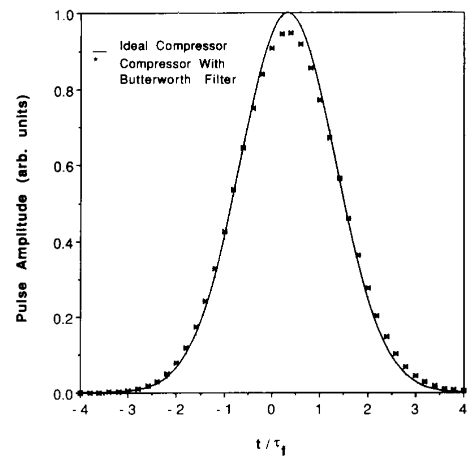

Fig. 1. Degradation in ideal pulse compression due to Butterworth filter.

Computer optimization techniques can be used to find the poles p_i and zeros z_i in (27) which yield the "best fit" to $H_c^{opt}(\omega)$ along the $j\omega$ axis. The optimum compression filter, given by (20), is an all-pass filter, since it has a constant magnitude independent of frequency. Thus, if a first-order Butterworth filter is included as discussed above, (27) may be rewritten as

$$H_c(\omega) = \frac{k}{1 + j(\omega - \omega_c)/\omega_0}\prod_{i=1}^{N}\frac{j(\omega - \omega_c) + p_i^*}{j(\omega - \omega_c) - p_i} \tag{28}$$

where * denotes complex conjugation and k is a constant. The poles p_i of the all pass filter can now be chosen by computer optimization to provide the required quadratic phase shift. Fortunately, the position of these poles will not affect the magnitude response of the filter. Thus, the design of the magnitude and phase responses have been decoupled.

IV. Waveguide Filters and the GLM Technique

Consider a corrugated waveguide filter consisting of a single-mode, planar channel waveguide, which has a quasi-periodic, corrugation etched into its top surface. The waveguide thickness can be written as

$$h(z) = h_0 + \Delta h(z)\cos\left(\frac{2\pi}{\Lambda_0}z + \Delta\phi(z)\right) \tag{29}$$

where h_0 is the nominal waveguide thickness, Λ_0 is the nominal corrugation period, $\Delta h(z)$ is the corrugation depth, and $\Delta\phi(z)$ is the phase deviation from perfect periodicity. Propagation through the filter can be modeled by the following pair of coupled-mode equations [13]

$$\frac{dB(z,\delta)}{dz} + jB(z,\delta) = q(z)A(z,\delta) \tag{30}$$

$$\frac{dA(z,\delta)}{dz} - j\delta A(z,\delta) = q^*(z)B(z,\delta) \tag{31}$$

where

$$\delta(\omega) = \beta(\omega) - \frac{\pi}{\Lambda_0} \tag{32}$$

$$q(z) = a(z) \exp(-j\Delta\phi(z)). \tag{33}$$

In (30)–(33), $A(z)$ and $B(z)$ are the electric field amplitudes, at frequency ω, of the backward and forward-propagating modes, respectively; $\beta(\omega) = \omega N_{\text{eff}}(\omega)/c$ is the propagation constant in the waveguide when $\Delta h(z) = 0$; and $a(z)$ is the coupling coefficient, which can be related to $\Delta h(z)$ by an overlap integral [13]. If we let

$$\Delta\omega = \omega - \omega_c \tag{34}$$

then, to first order, (32) becomes

$$\delta(\omega) = \left[\frac{\omega_c}{c} N_{\text{eff}}(\omega_c) - \frac{\pi}{\Lambda_0}\right] + \left[\frac{1}{c} N_{\text{eff}}(\omega_c) + \frac{\omega_c}{c}\frac{dN_{\text{eff}}(\omega_c)}{d\omega}\right]\Delta\omega \tag{35}$$

where N_{eff} is the waveguide effective index when $\Delta h(z) = 0$, and c is the speed of light in vacuum. We will assume that the nominal grating period has been chosen such that

$$\Lambda_0 = \frac{\pi c}{\omega_c N_{\text{eff}}(\omega_c)}. \tag{36}$$

Therefore,

$$\delta(\omega) = \left(\frac{N_{\text{eff}}(\omega_c)}{c} + \frac{\omega_c}{c}\frac{dN_{\text{eff}}(\omega_c)}{d\omega}\right)\Delta\omega. \tag{37}$$

The amplitude transfer function $r(\delta)$ of the filter measured in reflection is defined by

$$r(\delta) = \frac{A(0, \delta)}{B(0, \delta)}. \tag{38}$$

By direct substitution into the coupled-mode equations (30) and (31), it can be shown that if $r(\delta)$ corresponds to $q(z)$ and b is an arbitrary constant, then $r(\delta/b)$ corresponds to the new coupling coefficient $q(bz)/b$.

Given $r(\delta)$, the Gel'fand–Levitan–Marchenko (GLM) inverse scattering technique can be used to compute the coupling coefficient $q(z)$. The technique is described in reference 10 and is briefly outlined below. First, $r(\delta)$ is expressed in rational form

$$r(s) = \frac{N(s)}{D(s)} = \frac{\sum_{i=1}^{M} a_n s^n}{\sum_{n=1}^{N} b_n s^n} \qquad M < N \tag{39}$$

where $s = j\delta$, and the polynomial $\Delta(s)$ is computed

$$\Delta(s) = D(s)D^*(-s^*) - N(s)N^*(-s^*). \tag{40}$$

Note that $\Delta(s)$ is a polynomial of degree $2N$, and we denote its $2N$ roots by

$$\kappa_1, \kappa_2, \cdots \kappa_N \qquad -\kappa_1^*, -\kappa_2^*, \cdots, -\kappa_N^*.$$

It can be shown that the coupling coefficient $q(z)$ is given by

$$q(z) = -2 \lim_{s \to -\infty} sC_1(z, s) \exp(sz), \qquad z > 0 \tag{41}$$

where $C_1(z, s)$ is specified below

$$\begin{bmatrix} C_1(z, s) \\ C_2(z, s) \end{bmatrix} = -\frac{N(s)}{\Delta(s)}\left\{D^*(-s^*)\begin{bmatrix} 1 \\ 0 \end{bmatrix} + \begin{bmatrix} P_2^*(z, -s^*) \\ -P_1^*(z, -s^*) \end{bmatrix}\right\}\exp(sz) + \frac{1}{\Delta(s)}\left\{\begin{bmatrix} P_1(z, s) \\ P_2(z, s) \end{bmatrix} D^*(-s^*) - N(s) \cdot N^*(-s^*)\begin{bmatrix} 0 \\ 1 \end{bmatrix}\right\}\exp(-sz). \tag{42}$$

In (42), $P_1(z, s)$ and $P_2(z, s)$ are polynomials in s, of degree at most $N - 1$, for each value of z. Therefore, we can write

$$P_1(z, s) = \sum_{n=0}^{N-1} d_{1,n}(z)s^n \tag{43}$$

$$P_2(z, s) = \sum_{n=0}^{N-1} d_{2,n}(z)s^n. \tag{44}$$

Combining (39)–(44) yields the following simplified expression for the coupling coefficient $q(z)$ in terms of $d_{1,N-1}(z)$ and b_N.

$$q(z) = \frac{-2d_{1,N-1}(z)}{b_N}. \tag{45}$$

Finally, it can be shown that for each value of z, $C_1(z, s)$ and $C_2(z, s)$ are entire functions of s. Thus, $C_1,(z, s)$ and $C_2(z, s)$ have no poles in the complex s plane. Since κ_i, $i = 1, 2, \cdots, N$ is a root of $\Delta(s)$, and since $C_1(z, s)$ and $C_2(z, s)$ have no poles in the complex plane, it follows form (42) that

$$\begin{bmatrix} 0 \\ 0 \end{bmatrix} = -N(\kappa_i)\left\{D^*(-\kappa_i^*)\begin{bmatrix} 1 \\ 0 \end{bmatrix} + \begin{bmatrix} P_2^*(z, -\kappa_i^*) \\ -P_1^*(z, -\kappa_i^*) \end{bmatrix}\right\} \cdot \exp(\kappa_i z) + \left\{\begin{bmatrix} P_1(z, \kappa_i) \\ P_2(z, \kappa_i) \end{bmatrix} D^*(-\kappa_i^*) - N(\kappa_i)N^*(-\kappa_i^*)\begin{bmatrix} 0 \\ 1 \end{bmatrix}\right\}\exp(-\kappa_i z). \tag{46}$$

For each value of z, (46) represents $2N$ simultaneous linear equations ($i = 1, \cdots, N$) in $2N$ unknowns, $d_{1,0}(z), \cdots, d_{1,N-1}(z), d_{2,0}(z), \cdots, d_{2,N-1}(z)$, Once these equations are solved for $d_{1,N-1}(z)$, the coupling coefficient $q(z)$ may be computed from (45).

V. Pulse Compressor Design—An Example

In this section, the Gel'fand–Levitan–Marchenko inverse scattering technique is used to design a waveguide grating filter for pulse compression. We start by observing from (20) and (37) that the transfer function of the optimum pulse compressor, is given by

$$H_c^{opt}(\delta) = \exp\left[j4(C_c^2 - 1)^{1/2}\left(\frac{\delta}{\delta_0}\right)^2\right] \quad (47)$$

where

$$\delta_0 = |\delta(\omega_c + \omega_0)| \quad (48)$$

$$\omega_0 = \frac{2(2)^{1/2}}{\tau_f}. \quad (49)$$

This transfer function can be approximated by cascading a first-order Butterworth filter with an all-pass filter as noted in Section III. Thus, we write

$$H_c^{opt}(\delta) \approx H_c(\delta) = \frac{0.99}{1 + j\dfrac{\delta}{\delta_0}} \prod_{i=1}^{N} \frac{j\left(\dfrac{\delta}{\delta_0}\right) + \left(\dfrac{p_i^*}{\omega_0}\right)}{j\left(\dfrac{\delta}{\delta_0}\right) - \left(\dfrac{p_i}{\omega_0}\right)}. \quad (50)$$

This cascaded filter should produce nearly transform-limited compressed pulses as previously indicated in Fig. 1, since $\alpha_0 = \omega_0 \tau_f$ has been chosen to be $2(2)^{1/2}$. Also note from (37) that

$$\frac{\delta}{\delta_0} = \frac{\omega - \omega_c}{\omega_0}. \quad (51)$$

A compression ratio C_c of 3 is selected, and the poles p_i in (50) are chosen to minimize the phase difference between $H_c^{opt}(\delta)$ and $H_c(\delta)$ over the range $-0.6 < \delta/\delta_0 < 0.6$. This minimization is accomplished using a numerical optimization routine [14]. It is possible that the routine finds a local rather than global minimum. Linear and constant phase differences are ignored during the minimization, since these factors do not alter the pulse shape, but result only in a time delay. With a sixth-order all-pass filter (i.e., $N = 6$), a residual phase error of less than 0.06 radians is achieved over the range $-0.6 < \delta/\delta_0 < 0.6$. The poles p_i of the all-pass filter are given in Table I and Fig. 2, and a plot of the corresponding residual phase error is shown in Fig. 3(a) and (b). Note that Fig. 3(b) covers a larger range than Fig. 3(a), but is otherwise identical. The compressed pulse obtained using this all-pass filter is shown in Fig. 4. For comparison purposes, the optimum transform-limited compressed pulse is also shown. An examination of Figs. 1 and 4 indicates that the presence of the Butterworth filter, rather than the residual phase error, is the principal source of pulse shape degradation. Similar results were obtained using a fifth order all-pass filter. When four or less poles were used, however, the compressed pulse shape was degraded.

TABLE I
All-Pass Filter Pole Locations

p_1/ω_0	$-0.1368 - j0.6811$
p_2/ω_0	$-0.3214 + j0.2088$
p_3/ω_0	$-0.2002 - j0.5332$
p_4/ω_0	$-0.3912 - j0.5094$
p_5/ω_0	$-0.2781 - j0.0920$
p_6/ω_0	$-0.2457 - j0.3280$

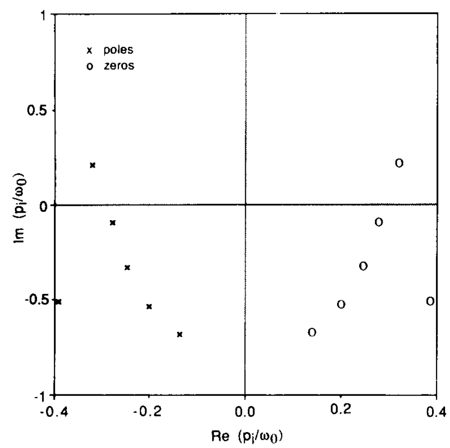

Fig. 2. All-pass filter pole/zero plot.

Given (50) and the pole locations specified in Table I, the Gel'fand–Levitan–Marchenko inverse scattering technique is used to determine the filter coupling coefficient $q(z)$. As noted in Section IV, application of this technique requires the solution of 12 (i.e., $2N$) simultaneous linear equations in 12 unknowns. The results are shown in Figs. 5 and 6 and are normalized by δ_o, which has units of reciprocal distance.

The performance of the pulse compressor described above can be compared to that of a linearly chirped waveguide grating filter. Ouellette [3], [4] has been shown that the phase response of such a filter is approximately quadratic in frequency, and thus this filter can be used for dispersion compensation and pulse compression. The grating frequency, $2\pi/\Lambda(z)$, of a linearly chirped filter can be written as

$$\frac{2\pi}{\Lambda(z)} = \frac{2\pi}{\Lambda_0 + \Delta\Lambda(z)} \approx \frac{2\pi}{\Lambda_0} - \frac{\Delta\Lambda(z)}{\Lambda_0^2}$$
$$= \frac{2\pi}{\Lambda_0} + \frac{F}{L^2}z, \quad -\frac{L}{2} \le z \le \frac{L}{2} \quad (52)$$

where L and Λ_0 are the length and nominal period of the grating, respectively, and F is the dimensionless chirp parameter. Using (52), the corresponding $\Delta\phi(z)$ in (33) becomes

$$\Delta\phi(z) = \int_{-L/2}^{z} \frac{F\xi}{L^2}\, d\xi = \frac{F}{8} + \frac{Fz^2}{2L^2}. \quad (53)$$

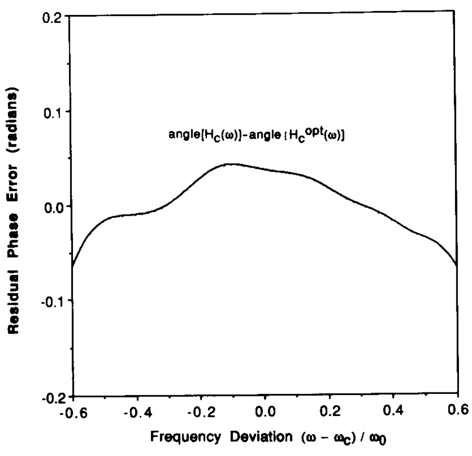

(a)

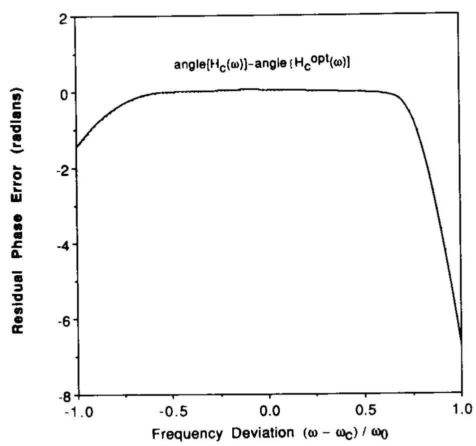

(b)

Fig. 3. (a) Pulse compressor residual phase error. (b) Pulse compressor residual phase error.

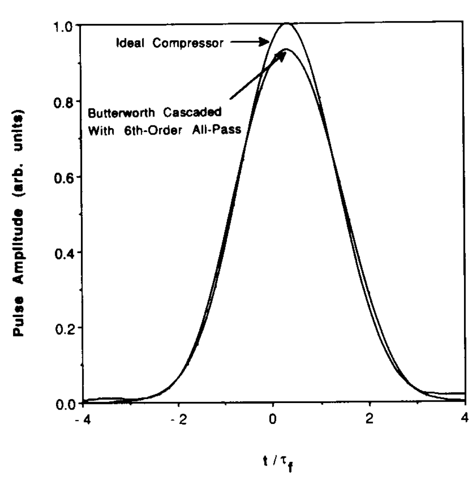

Fig. 4. Pulse compressor performance (GLM design).

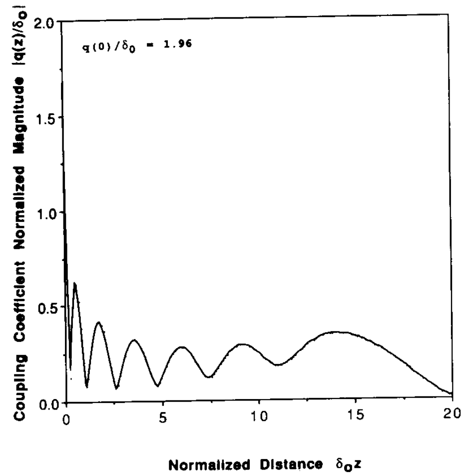

Fig. 5. Pulse compressor coupling coefficient (magnitude).

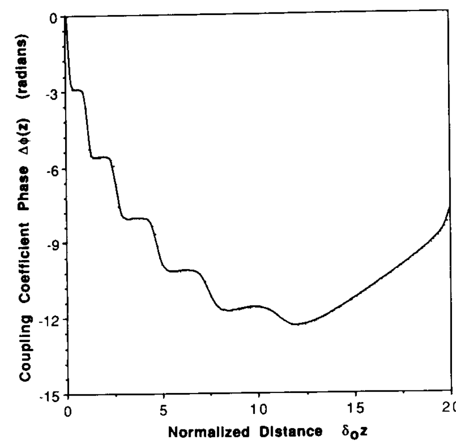

Fig. 6. Pulse compressor coupling coefficient (phase).

In [3], the magnitude of the coupling coefficient is chosen to be exponentially tapered, since this appears to improve the filter phase response. The coupling coefficient in (33) can then be written as

$$q(z) = \kappa \exp\left(-\frac{16z^2}{L^2}\right) \exp\left(-\frac{F}{8}\right) \exp\left(-\frac{Fz^2}{2L^2}\right) \quad (54)$$

where κ is a constant. For a given final pulsewidth τ_f the compression ratio C_c is a function of L^2/F as indicated below [3]

$$\frac{L^2}{F} \approx \frac{(C_c^2 - 1)^{1/2} c^2 \tau_f^2}{4N_{\mathrm{eff}}^2}. \quad (55)$$

In (55), N_{eff} is the effective index of the waveguide without the grating and is equal to $\lambda/(2\Lambda_0)$. We have computed the filter transfer function $r(\delta)$ by solving the coupled mode (30) and (31) numerically with $q(z)$ given by (54). Fig. 7 shows the result of using this filter to com-

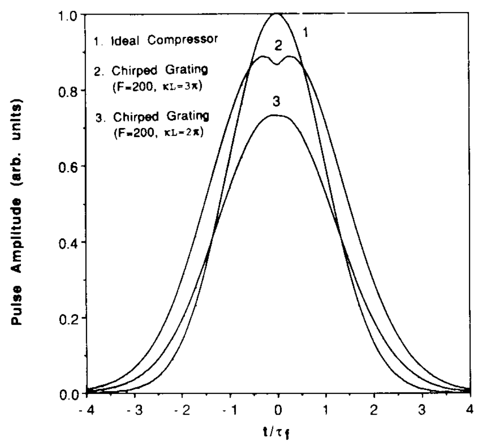

Fig. 7. Pulse compressor performance (linearly chirped waveguide grating filter design).

press a Gaussian pulse. A comparison of Figs. 4 and 7 indicates, as expected, that the GLM filter design technique produces a pulse which is more nearly transform-limited.

Fabrication of the filters described above is possible in principle, but would be difficult, since it requires precise control of both grating period and depth. As an example, we will assume that the filters are to be fabricated in a glass waveguide having an effective index N_{eff} equal to 1.5 at a wavelength of 1.55 μm. We will also make the reasonable assumption (for glass waveguides) that

$$\frac{\omega_c}{c}\frac{dN_{\text{eff}}(\omega_c)}{d\omega} << \frac{N_{\text{eff}}(\omega_c)}{c}.$$

Equations (24) and (37) can then be combined to yield

$$\delta_0 = \frac{N_{\text{eff}}(\omega_c)}{c}\frac{\alpha_0}{\tau_f}. \tag{56}$$

If the initial pulsewidth is 60 ps full width half maximum (i.e., $\tau_0 = 36$ ps) and if a compression ratio of 3 is desired, then the GLM-designed filter given in Figs. 5 and 6 has a length of approximately 17 mm and a maximum coupling coefficient of 2.36 mm^{-1}. A critical parameter in assessing the feasibility of fabricating such a filter is the maximum corrugation depth. If this depth is too large, than the coupled mode analysis used in this paper is no longer valid. For simplicity, we will consider a single-mode (TE), three layer, planar waveguide filter, since its coupling coefficient may be computed in closed form. The maximum value of the coupling coefficient for such a filter is given by [13]

$$\max|q(z)| = \frac{\pi}{\lambda}\frac{\max \Delta h(z)}{h_{\text{eff}}}\frac{n_f^2 - N_{\text{eff}}^2(\omega_c)}{N_{\text{eff}}(\omega_c)} \tag{57}$$

where n_f and h_{eff} are the refractive index and effective thickness of the waveguide layer, respectively. The values of n_f and n_f-$N_{\text{eff}}(\omega_c)$ for a typical glass waveguide formed by potassium thermal ion exchange will be on the order of 1.5 and 0.01, respectively. Thus for operation at a wavelength $\lambda_c = 1.55$ μm, and with max $|q(z)|$ equal to 2.36 mm^{-1}, (57) implies that the maximum fractional corrugation depth, max $(\Delta h(z)/h_{\text{eff}})$, will be approximately 5.8%. This value is small enough to justify our use of coupled mode theory.

For the same pulsewidth and compression ratio used above and with $N_{\text{eff}} \approx 1.5$, the linearly chirped grating filter corresponding to Fig. 7 has a length of 29 mm and a maximum coupling coefficient of either 0.216 or 0.325 mm^{-1}. The fractional change in grating period

$$\text{fractional change} = \frac{\Lambda(L/2) - \Lambda(-L/2)}{\Lambda_0} = \frac{F}{L}\Lambda_0 \tag{58}$$

is only 0.34%, and thus fabrication will be difficult. According to (55), the fractional change in grating period could be made larger by increasing both F and L. However, the length of the filter is already excessive.

In general, waveguide compression filters designed using either a chirped grating or the GLM technique have lengths proportional to the final pulsewidth. In addition, the peak coupling coefficient increases as the filter length decreases. Thus, it may be impractical to use waveguide compression filters in the femtosecond regime, since the required coupling coefficients will be large.

Finally, we note that it may be possible to design waveguide pulse compression filters by cascading together a series of purely periodic gratings spaced by appropriately long sections of waveguide [15], [16]. This cascaded approach uses only periodic gratings, and thus has the potential to simplify filter fabrication.

VI. Conclusion

Waveguide grating filters have been designed for pulse compression and dispersion compensation using the Gel'fand–Levitan–Marchenko inverse scattering technique. The transfer functions of these filters have a nearly perfect quadratic phase shift over the pulse bandwidth, and thus produce pulses which are close to transform-limited. The method employed illustrates a powerful technique for designing waveguide filters, with arbitrary magnitude and phase responses. The magnitude response is chosen first, and then the phase is controlled by cascading the filter with a rational all-pass network, whose poles are found by computer search. Using this method, a pulse compressor has been designed to compress a 60 ps pulse down to 20 ps. The waveguide grating parameters needed to fabricate the device have also been computed.

Appendix

The transfer function $H(\omega)$ of a first order Butterworth filter is

$$H(\omega) = \frac{1}{1 + j\dfrac{\omega}{\omega_0}}. \tag{A-1}$$

The impulse response $h(t)$ of this filter is the inverse Fourier transform of $H(\omega)$ and is given by

$$h(t) = \omega_0 \exp(-\omega_0 t) u(t) \tag{A-2}$$

where $u(t)$ is the unit step function. Let $g(t)$ denote the output of this filter when the input is $f(t)$. Then $g(t)$ is equal to the convolution of $f(t)$ with the filter impulse response $h(t)$. Therefore,

$$g(t) = \int_{-\infty}^{\infty} f(v) h(t - v)\, dv. \tag{A-3}$$

If $f(t)$ is the Gaussian pulse

$$f(t) = \exp\left(-\frac{t^2}{2\tau_f^2}\right) \tag{A-4}$$

then (A-2)–(A-4) may be combined to yield

$$g(t) = z_0 \exp(-z_0 \tau) \int_{-\infty}^{\tau} \exp\left(-\frac{u^2}{2}\right) \cdot \exp(z_0 u)\, du = z_0 \exp(-z_0 \tau) \cdot \exp\left(\frac{z_0^2}{2}\right) \int_{-\infty}^{\tau - z_0} \exp\left(-\frac{u^2}{2}\right) du \tag{A-5}$$

where

$$z_0 = \omega_0 \tau_f \tag{A-6}$$

$$\tau = \frac{t}{\tau_f}. \tag{A-7}$$

Equation (23) now immediately follows from the definition of the error function erf (x) and (A-5).

References

[1] G. P. Agrawal, *Nonlinear Fiber Optics*. Boston: Academic, 1989, ch. 6.

[2] J. Kuhl and J. Heppner, "Compression of femtosecond optical pulses with dielectric multilayer interferometers," *IEEE J. Quantum Electron.*, vol. QE-22, pp. 182–185, Jan. 1986.

[3] F. Ouellette, "Dispersion cancellation using linearly chirped Bragg grating filters in optical waveguides," *Opt. Lett.*, vol. 12, pp. 847–849, Oct. 1987.

[4] —, "All-fiber filter for efficient dispersion compensation," *Opt. Lett.*, vol. 16, pp. 303–305, Mar. 1991.

[5] H. G. Winful, "Pulse compression in optical fiber filters," *Appl. Phys. Lett.*, vol. 46, pp. 527–529, Mar. 1985.

[6] K. A. Winick and J. E. Roman, "Dispersion compensation and pulse compression using waveguide grating filters," presented at Ann. Meet. OSA, San Jose, CA, Nov. 3–8, 1991, paper MY7.

[7] D. K. Lam, B. K. Garside, and K. O. Hill, "Dispersion cancellation using optical fiber filters," *Opt. Lett.*, vol. 7, pp. 291–293, June 1982.

[8] A. H. Gnauck, L. J. Cimini, and L. W. Stulz, "Optical equalization of fiber chromatic dispersion in a 5-Gb/s transmission system," *IEEE Photon. Technol. Lett.*, vol. 2, pp. 585–587, Aug. 1990.

[9] F. Ouellette, "Limits of chirped pulse compression with an unchirped Bragg grating filter," *Appl. Opt.*, vol. 29, pp. 4826–4828, Nov. 1990.

[10] G.-H. Song and S.-Y. Shin, "Design of corrugated waveguide filters by the Gel'fand–Levitan–Marchenko inverse scattering method," *J. Opt. Soc. Amer.*, vol. 2, pp. 1905–1915, Nov. 1985.

[11] K. A. Winick, "Design of grating assisted waveguide couplers with weighted coupling," *J. Lightwave Technol.*, vol. 9, pp. 1481–1492, Nov. 1991.

[12] I. S. Gradshteyn and I. M. Ryzhik, *Table of Integrals, Series and Products*. Orlando, FL: Academic, 1980, p. 485.

[13] T. Tamir, Ed., *Guided-Wave Optoelectronics*. New York: Springer Verlag, 1988, Ch. 2.

[14] W. H. Press, P. P. Flannery, S. A. Teukolsky, and W. T. Vetterling, *Numerical Recipes*. Cambridge: Cambridge Univ., 1986, pp. 521–528.

[15] H. Haus, private communications.

[16] H. Haus and R. V. Schmidt, "Transmission response of cascaded gratings," *IEEE Trans. Sonics and Ultrason.*, vol. SU-24, pp. 94–101, Mar. 1977.

Jose E. Roman was born in San Juan, Puerto Rico, in 1965. He received the B.S. degree in electrical engineering from the University of Florida, Gainesville, in 1987, and the M.S. degree from the University of Michigan, Ann Arbor, in 1989.

Currently, he is pursuing the Ph.D. degree in electrical engineering at the University of Michigan. His area of interest is integrated optics.

Mr. Roman is a member of the Optical Society of America.

Kim A. Winick (S'77–M'80) was born in New York City, NY, on July 27, 1954. He received the B.S. degree in electrical engineering from the Pennsylvania State University, University Park, in 1976, and the M.S. and Ph.D. degrees in electrical engineering from the University of Michigan, Ann Arbor, in 1977 and 1981, respectively. While at the University of Michigan, he held a National Science Foundation Graduate Fellowship.

From 1981 until 1988, he was a technical staff member at Lincoln Laboratory, Massachusetts Institute of Technology, Lexington, working on millimeter wave and coherent optical communications systems. Since Autumn 1988, he has been an Assistant Professor with the Department of Electrical Engineering and Computer Science, University of Michigan. His major research interests are in the area of integrated optics and communications.

Dr. Winick is a member of the Optical Society of America.